EDGE ARTICLE

Check for updates

Triplet energy transfer from quantum dots increases Ln(III) photoluminescence, enabling excitation at visible wavelengths†

Tingting Huang, [‡a] Sheng He,[‡b] Anji Ni,[b] Tianquan Lian [*b] and Ming Lee Tang [*a]

Europium(III) complexes are promising for bioimaging because of their long-lived, narrow emission. The photoluminescence (PL) from europium(III) complexes is usually low. Thus, the effective utilization of low-energy light >400 nm and enhancement of PL are long-standing goals. Here, we show for the first time that 1-naphthoic acid triplet transmitter ligands bound to CdS quantum dots (QDs) and europium(III) complexes create an energy transfer cascade that takes advantage of the strong QD absorption. This is confirmed by transient absorption spectroscopy, which shows hole mediated triplet energy transfer from QDs to 1-NCA, followed by triplet transfer from 1-NCA to europium(III) complexes with an efficiency of $65.9 \pm 7.7\%$. Smaller CdS QDs with a larger driving force lead to higher triplet transfer efficiency, with Eu(III) PL intensity enhanced up to 21.4 times, the highest value ever reported. This hybrid QD system introduces an innovative approach to enhance the brightness of europium complexes.

Introduction

Lanthanide(III) (Ln) ions have attracted much attention because their unique properties enable various applications, such as bioimaging,[1,2] electroluminescence displays, lasers, sensors, and light-emitting diodes.[3] Europium(III) ions are notable in the lanthanide family because of their sharp photoluminescence peaks, large Stokes shift and micro- to milli-second lifetimes.[4,5] Unfortunately, the direct photoexcitation of lanthanide ions is very inefficient, due to the intrinsically low absorption coefficients, and the large intramolecular or environmental-based loss processes. Hence, it is critical to improve the photoluminescence (PL) efficiency of Eu(III) ions.

Direct band gap quantum dots (QDs) have been recognized as potential sensitizers for Eu^{3+} ions due to the strong broadband absorption above the QD band gap. Due to quantum confinement, the QD bandgap is easily tuned by size, shape, composition, and shell material. One strategy to utilize QDs for enhancing Ln photoluminescence is by doping Ln^{3+} ions into QDs. For example, Yb^{3+} ions on the surface of CdSe QDs can accept energy from the QDs, resulting in a NIR emission from the Yb^{3+} $^2F_{5/2}$ state, although no values for the photoluminescence quantum yield (PLQY) were reported.[6] Europium-doped CdS QDs showed two Eu^{3+} local coordination sites attributed to surface and interior sites.[7] ZnS and CdS nanoparticles doped with Tb^{3+} and Eu^{3+} on the surface have also been reported.[8] CdSe semiconductor nanocrystals have been used to sensitize Tb^{3+} by incorporation of Tb^{3+} cations into the nanocrystals during synthesis.[9] A downshifting configuration combined the broad absorption of InP with the narrow emission of the Ln^{3+} ion in core/shell/shell $InP/Ln_xY_{1-x}F_3/ShF_3$ (Ln = Yb, Nd; Sh = Lu, Y).[10] These synthesis methods are complicated by the fact that Ln^{3+} ions are hard acids and incompatible with the softer ionic lattice of prototypical II–VI materials. Recently, there has been a significant increase in the utilization of halide perovskite nanocrystals for Ln^{3+} doping. However, challenges related to chemical stability, toxicity, and limited light absorption still persist.[11,12] Furthermore, the exact mechanism of energy transfer in Ln^{3+}-doped quantum dots remains unclear.

Another traditional method for improving the PL efficiency of Eu^{3+} involves intramolecular energy transfer between coordinating organic ligands and central ions.[13] The commonly accepted sensitization mechanism includes intersystem crossing between the ligand singlet and triplet excited states and the triplet transfer from the ligand T_1 to the Eu^{3+} center. Generally, the efficiency of triplet energy transfer depends on the overlap between the lowest triplet energies of the ligand and the resonant $^5D_0$ emitting levels of Eu^{3+}, which is 17 500 cm^{-1}.[14,15] Therefore, the singlet state of the antenna ligand needs to be in the UV region. Hence, organometallic Eu^{3+} complexes typically do not absorb wavelengths red of 400 nm

aDepartment of Chemistry, University of Utah, Salt Lake City, UT, 84112, USA. E-mail: minglee.tang@utah.edu

bDepartment of Chemistry, Emory University, 1515 Dickey Drive Northeast, Atlanta, Georgia 30322, USA. E-mail: tlian@emory.edu

† Electronic supplementary information (ESI) available: Experimental methods, synthesis, data fitting procedures and computational details. See DOI: https://doi.org/10.1039/d3sc05408j

‡ T. H. and S. H. contributed equally to this paper.

because most of the antenna ligands are transparent in this region.[16] Efforts to address this limitation include controlling energy levels of donor ligands,[17] designing coordination structures through varying ligand field symmetry[18] and coordination number,[4,19] and hybrid material research on the transfer of energy from external sources to Eu^{3+} complexes. Previous studies showed energy transfer to Eu^{3+} complexes by Förster resonance energy transfer (FRET).[20,21] For example, FRET was used to describe the enhancement of PL from a naphthalene functionalized Eu^{3+} complex whose absorption overlapped with the emission of the conjugated polymer donor.[17] Nanoparticles like ZnS[22] and InPZnS@ZnSe/ZnS[23] with surface-modified Ln(III) were synthesized. Still, none of these examples enabled low energy excitation with visible wavelengths >400 nm for Ln(III), nor showed triplet energy transfer between QDs and Ln(III) complexes. Separately, Miyata and Onda improved PL by three orders of magnitude using a triplet transporting host whose donor T_1 level matched the acceptor levels of an organometallic Eu(III) dopant.[24] We note that the most red-shifted excitation so far for Eu(III) complexes can be found in the recent work by Hasegawa et al. utilizing a pair of stacked coronenes where the intramolecular π–π interactions create a low-energy excimer to photosensitize Eu^{3+} centers with 450 nm light.[25]

In order to utilize the strong broadband absorption of QDs for subsequent triplet energy transfer,[26,27] we and others have demonstrated the application of the QD sensitized three-component system (namely the QD triplet photosensitizer, transmitter, and triplet acceptor/emitter).[28–31] In this work, we show for the first time that organometallic lanthanide complexes can be sensitized by making use of the large absorption cross-section of CdS QDs and transmitter ligands like the QD sensitized three-component system. We find that QDs enhance the narrow emission from a Eu{(+)-facam}$_3$ molecule 21-fold compared to the pure molecule, and smaller CdS QDs enhance the Eu{(+)-facam}$_3$ emission more. Transient absorption reveals a hole mediated triplet energy transfer from CdS QDs to the transmitter, and a 65.9 ± 7.7% efficiency of triplet transfer from the transmitter to Eu{(+)-facam}$_3$. Compared to the stacked coronenes,[25] we observe a similar 5-fold enhancement with blue excitation. However, using CdS QD photosensitizers presents several advantages. Unlike an excimeric 442 nm absorption band, QDs have a higher extinction coefficient. This feature enhances light absorption and energy transfer efficiency. Moreover, our system offers greater flexibility with the ability to combine different QDs with different Ln^{3+} complexes because of the clear triplet-based mechanism. Our downshifting configuration exploits the size tunability of QDs and provides a guide for future work enhancing the emission of organometallic lanthanide complexes.

Results and discussion

In this hybrid system, the band edge exciton of CdS QDs is transferred to the T_1 state of the 1-naphthoic acid (1-NCA) transmitter ligand, then to the emitter Eu{(+)-facam}$_3$. The latter emits at 613 nm in the red, i.e., the Eu^{3+} $^5D_0$ to $^7F_2$ transition. Multiple emission peaks of Eu{(+)-facam}$_3$ were observed

at 579, 585–600 and 613 nm; they are assignable to the $^5D_0 \rightarrow$ $^7F_0$, $^5D_0 \rightarrow$ $^7F_1$ and $^5D_0 \rightarrow$ $^7F_2$ transition of Eu(III) ions.[32] Fig. 1a depicts triplet energy transfer from cadmium chalcogenide QDs to Eu{(+)-facam}$_3$. CdS QDs of 3.55–5.05 nm diameter[33] (Table S1†) are used as triplet photosensitizers because their size-dependent band gaps between 2.78 and 3.06 eV (or 405–445 nm) allow energy transfer to the $^5D_0$ level of Eu^{3+} (2.16 eV). In this hybrid system, it is expected that the QD band edge exciton states, containing both spin singlet and triplet character,[34] transfer energy to the T_1 state of 1-NCA, then to the emitter Eu{(+)-facam}$_3$. Ideal transmitter ligands must have a suitable T_1 energy that is higher than the $^5D_0$ level of Eu^{3+} and lower than QD band-edge excitons for efficient Dexter energy transfer to Eu{(+)-facam}$_3$. 1-NCA with its T_1 state of 2.5 eV satisfies these requirements as shown in Fig. 1a. In addition, 1-NCA also has a carboxylic acid group for direct attachment to the CdS QD surface to promote the necessary orbital overlap. Here we choose to directly mix the 1-NCA with CdS QDs without further purification because non-bound 1-NCA serves as diffusive triplet energy relays and shows better outcomes than the removal of excess ligands through washing.[27] The complex that resulted from mixing 7.5 mM 1-NCA and 2.5–9.9 × 10^{-1} μM CdS QDs in toluene is labeled as CdS/1-NCA. Eu{(+)-facam}$_3$ is directly added into the CdS/1-NCA solution, resulting in a final concentration of 1.23 mM. Details of sample preparation are provided in ESI Sections 2.1–2.3 with Fig. S1 and Table S2.† Fig. 1b shows the absorption and photoluminescence of each component in the system. Compared to the absorption of 1-NCA and Eu{(+)-facam}$_3$, the longer wavelength (>400 nm) absorption onset of CdS QDs enables the sensitization of Eu{(+)-facam}$_3$ by lower energy photons, as will be discussed below.

The role of each component in the hybrid system was examined and the enhancement subsequently measured. Fig. 2a shows the comparison of PL spectra with 416 nm excitation at the same power for four samples of 1.23 mM of Eu{(+)-facam}$_3$ in pure toluene (black), mixed with oleic acid capped CdS only (blue), mixed with 1-NCA only (green), and with CdS/1-NCA (red). Pure Eu{(+)-facam}$_3$ in toluene shows negligible PL because it has negligible absorption at this wavelength. When CdS QDs capped with native oleic acid ligands are introduced, other than the broad trap state emission of CdS QDs (blue), no enhanced emission from Eu{(+)-facam}$_3$ is observed. This indicates inefficient triplet energy transfer from the CdS donor directly to the Eu{(+)-facam}$_3$ acceptor. This is due to the long insulating aliphatic chains on CdS, which exceed the Dexter radius. A small increase of the 613 nm PL by mixing Eu{(+)-facam}$_3$ with 1-NCA in toluene (without CdS, green line) is observed, which is attributed to the effect of coordinating 1-NCA to Eu^{3+}. The intensity of Eu^{3+} emission has been reported to be proportional to the coordinative strength of the solvent where weakly coordinating solvents such as toluene give lower emission compared to strongly coordinating solvents like dimethyl sulfoxide and dimethylformamide.[35] Although with UV excitation, 1-NCA can also photosensitize the Eu^{3+} center, this possibility can be excluded with the 416 nm excitation used here, which cannot excite 1-NCA.[36] Finally, the
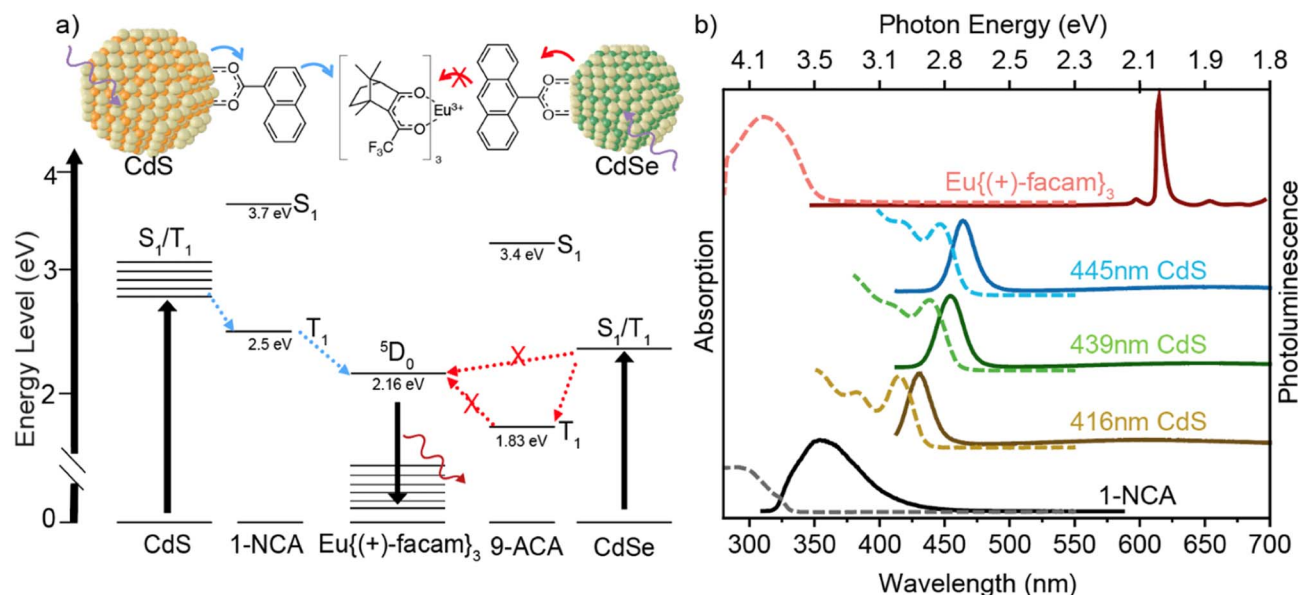
Fig. 1 (a) Schematic of energy transfer. The CdS nanocrystals functionalized with a 1-naphthoic acid (1-NCA) transmitter ligand. Eu{(+)-facam}$_3$ serves as the emitter. The purple arrow indicates photoexcitation of CdS QDs of different sizes, followed by energy transfer from CdS to 1-NCA and from 1-NCA to Eu{(+)-facam}$_3$. The right half illustrates the unfavored sensitization using CdSe QDs and 9-anthracene carboxylic acid (9-ACA). (b) Absorption (dashed line) and photoluminescence spectra (solid line) of Eu{(+)-facam}$_3$, 416 nm/439 nm/445 nm absorbing CdS QDs, and 1-NCA from top to bottom, measured in toluene at RT. The excitation wavelengths are 405 nm for the top four samples and 300 nm for 1-NCA.

highest Eu{(+)-facam}$_3$ emission is observed when it is mixed with CdS/1-NCA (red), where the 1-NCA ligand on the CdS nanocrystal creates an energy cascade between the CdS donor and Eu{(+)-facam}$_3$ acceptor, as expected from Fig. 1a. For simplicity, we will also refer to this sample as CdS/NCA/Eu hereafter.

We first quantify the effect of CdS QD photosensitization by measuring the PL intensity enhancement, which is defined as

$$\text{PL enhancement} = I_{\text{PL}}^{\text{CdS/1-NCA}} / I_{\text{PL}}^{\text{1-NCA only}} \qquad (1)$$

In eqn (1), $I_{\text{PL}}^{\text{CdS/1-NCA}}$ and $I_{\text{PL}}^{\text{1-NCA only}}$ represent the PL intensity at 613 nm of 1.23 mM Eu{(+)-facam}$_3$ in the presence of the CdS/1-NCA photosensitizer or 1-NCA only in toluene, respectively. The PL intensity enhancement can be caused by both enhanced absorption at the excitation wavelength and PL quantum yield (QY) of the Eu center in the presence of CdS QDs. Here we have used 1.23 mM Eu{(+)-facam}$_3$/1-NCA toluene as the reference sample for the calculation of the PL enhancement factor by the QDs because, as discussed above, 1-NCA can also enhance the Eu PL. We measured the PL enhancement factors for four CdS QDs with band edge absorption at 416, 435, 439, and 445 nm,
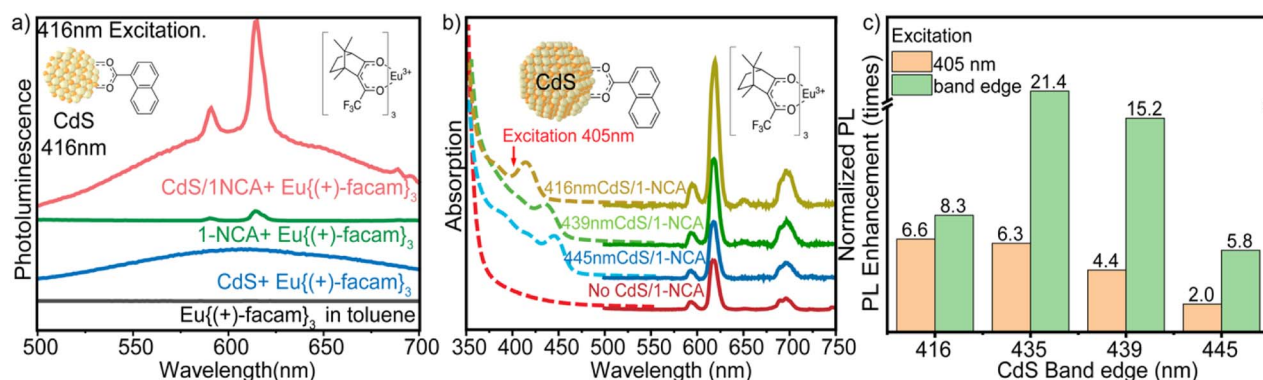
Fig. 2 (a) Photoluminescence spectra with excitation at the CdS band edge with 416 nm CW light from the fluorimeter. (b) Absorption (dashed line) and photoluminescence spectra (solid line) of 1.23 mM Eu{(+)-facam}$_3$ with 416 nm/439 nm/445 nm absorption maxima CdS/1-NCA or in 1-NCA/toluene with excitation of 405 nm, measurements were performed at room temperature (RT). The Eu{(+)-facam}$_3$ PL spectra were obtained by subtracting the CdS/1-NCA trap state emission (raw data in Fig. S2†). (c) PL enhancement with different sizes of CdS excited at 405 nm (orange column) and at the CdS band edge (green column). See text for details.

referred to as CdS416, CdS435, CdS439, and CdS445, respectively. The absorption spectra of CdS/1-NCA/Eu samples of CdS416, CdS439 and CdS445 are compared in Fig. 2b. Also shown in Fig. S2† and 2b is a comparison of the PL spectra of these samples measured with 405 nm excitation. As shown in Fig. S2,† the raw PL spectra show both a broad CdS QD trap state emission and the sharp Eu emission. The former can be subtracted from the total emission by comparing with the emission spectra of QD/1-NCA (without the Eu) and only the Eu emission is shown in Fig. 2b. The comparison shows that all these QDs enhance the PL emission of the Eu center compared to the 1-NCA/Eu sample. Fig. 2c summarizes the enhancement factors calculated from eqn (1), which shows that for 405 nm excitation, the enhancement factors decrease from 6.6 to 2.0 when increasing the QD size from 416 nm to 445 nm. This indicates that the driving force and coupling strength for triplet energy transfer from QD to 1-NCA, both decrease at large QD sizes, and may be a key factor for the overall enhancement of Eu {(+)-facam}$_3$ emission. The results agree with previous reports in the literature that CdS to 1-NCA triplet energy transfer (TET) efficiency is correlated with the driving force between QDs and the surface bound mediator. The larger driving force for TET from a smaller QD provides a higher triplet transfer efficiency.[27] We and others have shown that this first TET step is strongly correlated with the NC size, e.g., with PbS, PbSe[37,38] or CdSe/9-ACA triplet photosensitizers.[39,40] Here, we have also measured the enhancement factor for these QDs with excitation at their band edge absorption. As shown in Fig. 2c, the CdS/1-NCA photosensitizers enhanced the PL of Eu{(+)-facam}$_3$ by a factor of 8.3, 21.4, 15.2 and 5.8 for CdS416, CdS435, CdS439 and CdS445, respectively. These enhancement factors are larger than those measured at 405 nm excitation, because $I_{PL}^{1-NCA\ only}$ decreases at longer excitation wavelength due to the diminishing Eu absorption, as shown in Fig. S3.†

To quantify the contributions of enhanced absorption and PLQY to the measured total PL intensity enhancement, we also determine the PLQY enhancement factors by accounting for the wavelength dependent sample absorption. The definition of PLQY of the hybrid systems is given by eqn (S1)† and the measurement details are provided in the ESI.† In short, the PLQY is determined by scaling the total PL intensity of the hybrid system by the number of absorbed excitation photons and by comparing to the QY of a standard sample, 4-(dicyanomethylene)-2-methyl-6-(4-dimethylaminostyryl)-4H-pyran (DCM), which has a known quantum yield of 30% in methanol.[41] The measured PLQYs for both 405 nm and band edge excitation are listed in Table S3.† For example, the CdS416/1-NCA/Eu system has the maximum PLQY of 0.118%, which is 3 times larger than the PLQY of Eu{(+)-facam}$_3$ in 1-NCA/toluene (0.036%). This result indicates efficient triplet energy transfer from the excited QDs to 1-NCA and to the Eu center, as depicted in Fig. 1a, and the quantum efficiency of this photosensitization scheme for generating the Eu emissive state is higher than that of the direct excitation of the Eu{(+)-facam}$_3$/1-NCA complexes.

Two potential hybrid systems, one using CdSe/9-ACA, the other using CdS/ZnS core/shell QDs as triplet photosensitizers were also examined to further investigate the role of triplet

energy transfer from the QDs. As shown in Fig. 1a, 9-anthracene carboxylic acid (9-ACA) has a T_1 level at 1.8 eV, lower than that of 1-NCA, and the bandgap of the CdSe QDs is at 2.37 eV (524 nm), also smaller than that compared to CdS.[42,43] There was no PL enhancement from these CdSe QDs to the emitter Eu {(+)-facam}$_3$ either directly from CdSe or through the 9-ACA transmitter ligand (Fig. S4†). This is because the energy level of 9-ACA (1.83 eV) is lower than $^5D_0$ (2.16 eV) and the energy transfer from 9-ACA to europium is thermodynamically uphill (Fig. 1a). This result suggests the importance of triplet energy in the QD sensitization scheme reported here. CdS/ZnS core/shell nanostructures were also used to replace the CdS QDs in this hybrid system. CdS/ZnS core shell QDs were made from a 416 nm absorption maxima CdS core (Fig. S5†). After shelling, a 15 nm redshift was observed in absorption and PL due to 3 monolayers of ZnS shell (as confirmed by ICP spectroscopy). Unfortunately, this CdS/ZnS core/shell structure only showed a 2.1-fold PL enhancement in Eu(ɪɪɪ) 613 nm emission, which is lower than the 6.6 times PL enhancement using the original 416 nm CdS core. Though this shell passivates surface trap states, it might be too thick, slowing down the triplet energy transfer from the QDs to NCA.[44]

Transient absorption (TA) confirms that efficient TET between CdS QDs, 1-NCA, and Eu{(+)-facam}$_3$ is responsible for the PL enhancement. CdS QDs with 416 nm 1S exciton transition were selected for these studies since they show the highest PL enhancement as discussed above with 405 nm excitation. TA spectra at indicated delay times after 400 nm excitation of CdS QD, CdS/1-NCA, and CdS/1-NCA + Eu{(+)-facam}$_3$ are summarized in Fig. S6.† Fig. 3 shows the 2D pseudocolor TA spectra of all three samples. At <1 μs, the TA spectra are dominated by the CdS QD signals, including the exciton bleach (XB) centered around 413 nm caused by the band edge electron, the positive photo-induced absorption (PA) peaks on both sides of XB due to the Stark effect, and a broad PA signal spanning from 500 nm to 700 nm (Fig. S6† and insets) due to trapped hole absorption.[45,46] Comparison of Fig. S6d–f† shows that the trapped hole signal decays faster with the addition of 1-NCA. The kinetics are discussed below. In CdS only samples (Fig. 3a), the CdS QD signals decay to zero at ~1 μs due to electron–hole recombination, while in CdS/1-NCA (Fig. 3b), the positive absorption signal centered at 435 nm persists at >1 μs. This can be clearly seen in Fig. S6e† inset, which shows that although this additional long-lived signal in CdS/1-NCA overlaps with the Stark effect induced PA signal in pure CdS QDs, it lives much longer than the PA signal in the CdS only sample. This longer-lived positive signal in the presence of 1-NCA is attributed to the T_1-to-T_n transition of the 1-NCA triplet state, ^{3}NCA*, according to the literature.[47–49] Interestingly, this ^{3}NCA* signal decays faster with the addition of Eu{(+)-facam}$_3$ (Fig. 3c and S6f† inset), which can be attributed to TET from ^{3}NCA* to Eu{(+)-facam}$_3$.

To obtain the formation and decay kinetics of ^{3}NCA*, the overlapping CdS QD signals in the TA spectra of CdS/1-NCA and CdS/1-NCA + Eu{(+)-facam}$_3$ were subtracted, resulting in the double difference TA spectra shown in Fig. S7.† Details of the subtraction are given in the ESI, Section 2.5.† The ^{3}NCA* kinetics in CdS/1-NCA extracted from Fig. S7b† and the
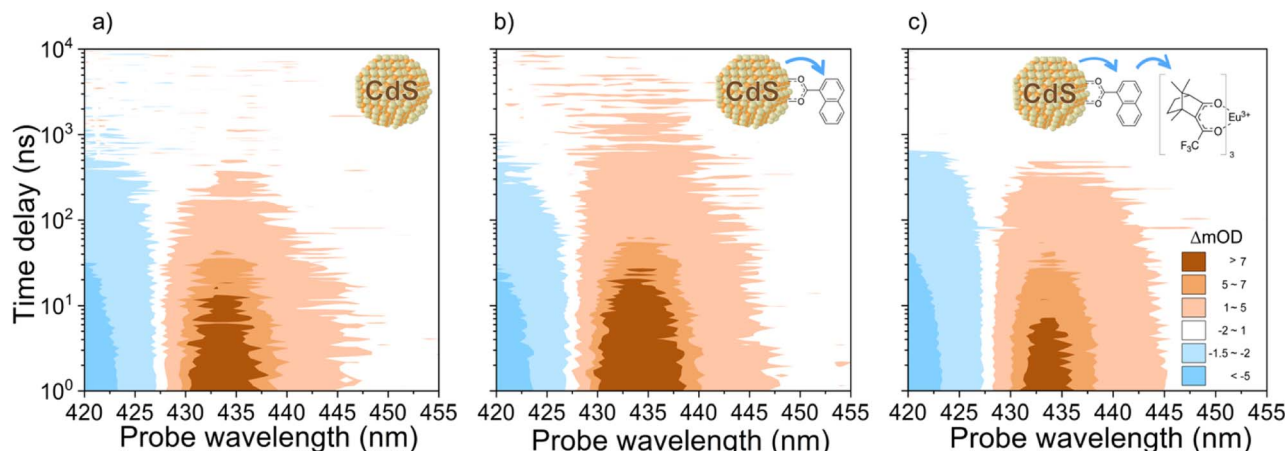
Fig. 3 Transient absorption (TA) spectra measured at 400 nm excitation for (a) CdS416, (b) CdS416/1-NCA only, and (c) CdS416/1-NCA with 1.23 mM Eu{(+)-facam}$_3$. Comparison of (a) and (b) shows that the long-lived naphthalene triplet absorption at 430–440 nm is observed at >1 µs in CdS/1-NCA, indicating TET from CdS* to NCA to form ^{3}NCA*. Comparison of (b) and (c) shows that the naphthalene triplet absorption decays faster in the presence of Eu{(+)-facam}$_3$, indicating TET from ^{3}NCA* to Eu{(+)-facam}$_3$. All samples are in toluene at RT.

corresponding CdS QD signal kinetics are compared in Fig. 4a. As discussed above, the trapped hole kinetics in CdS/1-NCA shows a faster decay than that in pure CdS QDs, indicating hole transfer to 1-NCA. Note that the corresponding 1-NCA cation signal which should appear in the near IR region was not observed in the current detection wavelength range.[47] After the trapped hole decay, >20 ns, the ^{3}NCA* signal starts to increase, together with a slightly faster decay of the XB in CdS/1-NCA compared to the XB in pure QD, suggesting electron transfer from CdS to 1-NCA. These well separated hole transfer, electron transfer, and triplet formation kinetics together suggest hole mediated TET from CdS QDs to 1-NCA, similar to observations in CsPbBr$_3$ nanocrystals and PbS QDs.[47,50,51] Similar kinetics were measured for CdS/1-NCA + Eu{(+)-facam}$_3$, as shown in Fig. S9.† Fitting the kinetics to the hole transfer mediated TET mechanism (ESI, Section 3†) gives the hole transfer rate

constant of 0.111 ± 0.005 ns^{-1} and the hole transfer efficiency of $74.1 \pm 1.1\%$. The ^{3}NCA* formation and decay rate constants are 68 ± 1 µs^{-1} and 99.5 ± 17.3 ms^{-1}, respectively. In addition, the QD-to-1-NCA TET efficiency is also estimated according to the TA signal amplitudes of ^{3}NCA* and CdS XB, and corresponding extinction coefficients (ESI, Section 4†), which result in a TET efficiency of 74.4%, close to the hole transfer efficiency. This consistency suggests that 1-NCA triplet formation is the major decay pathway of the charge separated state CdS$^-$/1-NCA$^+$. Fig. 4b compares the ^{3}NCA* kinetics in CdS/1-NCA and CdS/1-NCA + Eu{(+)-facam}$_3$. While the formation kinetics are the same in both samples, the decay rate constant of ^{3}NCA* increases from 99.5 ± 17.3 ms^{-1} to 291.8 ± 42.4 ms^{-1} with Eu{(+)-facam}$_3$, consistent with TET from 1-NCA to Eu{(+)-facam}$_3$. From the decay rate constants, the TET efficiency is calculated to be $65.9 \pm 7.7\%$.
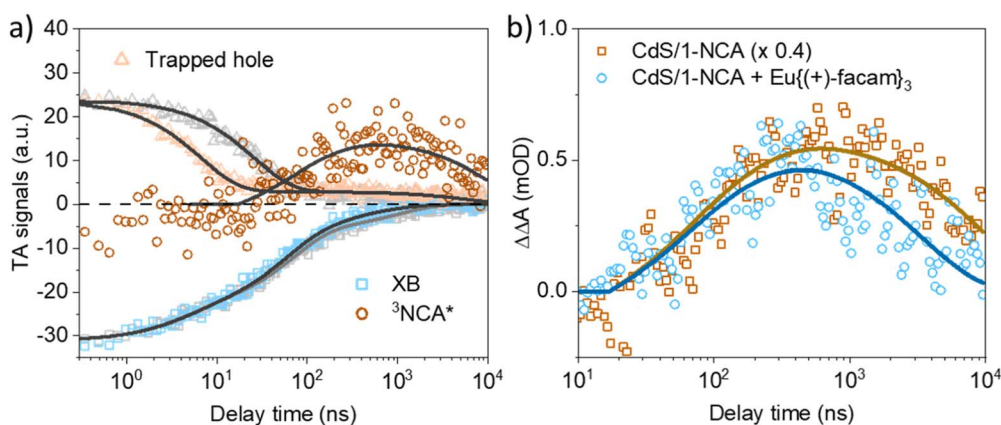

Fig. 4 (a) TA kinetics of trapped hole (orange triangles), XB (blue squares), and ^{3}NCA* (brown circles) in the CdS/1-NCA sample. Also shown for comparison are the kinetics of trapped holes (grey triangles) and XB (grey squares) in pure CdS QDs. The trapped hole and ^{3}NCA* kinetics are scaled for better comparison. Solid lines represent the fitting curves discussed in the ESI, Section 3.† Note that the light grey line is the fitting to the XB kinetics of pure CdS QDs. (b) ^{3}NCA* kinetics in CdS/1-NCA (brown square) and CdS/1-NCA + Eu{(+)-facam}$_3$ (cyan circle) extracted from the double difference TA spectra (ΔΔ*A*) Fig. S7b and c.† The colored solid lines are the fitting curves. mOD: milli-optical density.

Conclusions

To conclude, a new method for enhancing Eu{(+)-facam}$_3$ emission with a hybrid system using a transmitter ligand for triplet energy transfer from quantum dots is presented. Transient absorption shows that TET occurs from CdS/1-NCA to Eu{(+)-facam}$_3$ with a rate of 192.3 ± 45.8 ms^{-1} and efficiency of $65.9 \pm 7.7\%$. Smaller CdS with a larger driving force leads to higher triplet energy transfer efficiency. The utilization of a QD-based hybrid system, comprising π-conjugated molecules as a bridge and Ln(III) complex emitters, offers an excellent approach to significantly enhance the photoluminescence intensity of Ln(III) complexes. For example, QDs can enhance the emission of Ln(III) complexes located in the visible to NIR range, e.g., $^4G_{5/2}$ of Sm^{3+} (17 800 cm^{-1}), $^5D_4$ of Tb^{3+} (20 400 cm^{-1}) and $^3P_0$ of Pr^{3+} (20 473 cm^{-1}). More importantly, enhancing the emission of chiral Ln molecules can potentially develop applications in optical sensors, lasers, and organic photoelectric devices for 3D displays.[52] This work provides a guide to understanding, designing, and synthesizing functional hybrid nanoparticle systems that can enhance the molecular PL of Ln^{3+} complexes.

Data availability

All experimental data are available from the corresponding author upon reasonable request.

Author contributions

T. H. designed and executed the ligand exchange, electronic absorption and photoluminescence quantum yield measurements. S. H. conducted the transient absorption measurements, spectra and kinetics analysis. A. N. contirbuted to transient absorption spectra analysis. The manuscript was written through contributions from T. H., S. H., M. L. T. and T. L.

Conflicts of interest

There are no conflicts to declare.

Acknowledgements

References

1 F. Vetrone, R. Naccache, A. Zamarrón, A. Juarranz de la Fuente, F. Sanz-Rodríguez, L. Martinez Maestro, E. Martín Rodriguez, D. Jaque, J. García Solé and J. A. Capobianco, Temperature Sensing Using Fluorescent Nanothermometers, *ACS Nano*, 2010, **4**(6), 3254–3258.

2 F. S. Richardson, Terbium(III) and europium(III) ions as luminescent probes and stains for biomolecular systems, *Chem. Rev.*, 1982, **82**(5), 541–552.

3 R. D. Costa, E. Ortí, H. J. Bolink, F. Monti, G. Accorsi and N. Armaroli, Luminescent Ionic Transition-Metal Complexes for Light-Emitting Electrochemical Cells, *Angew. Chem., Int. Ed.*, 2012, **51**(33), 8178–8211.

4 T. Harada, H. Tsumatori, K. Nishiyama, J. Yuasa, Y. Hasegawa and T. Kawai, Nona-Coordinated Chiral Eu(III) Complexes with Stereoselective Ligand–Ligand Noncovalent Interactions for Enhanced Circularly Polarized Luminescence, *Inorg. Chem.*, 2012, **51**(12), 6476–6485.

5 M.-a. Morikawa, S. Tsunofuri and N. Kimizuka, Controlled Self-Assembly and Luminescence Characteristics of Eu(III) Complexes in Binary Aqueous/Organic Media, *Langmuir*, 2013, **29**(42), 12930–12935.

6 R. Martin-Rodriguez, R. Geitenbeek and A. Meijerink, Incorporation and luminescence of Yb3+ in CdSe nanocrystals, *J. Am. Chem. Soc.*, 2013, **135**(37), 13668–13671.

7 J. Planelles-Aragó, E. Cordoncillo, R. A. S. Ferreira, L. D. Carlos and P. Escribano, Synthesis, characterization and optical studies on lanthanide-doped CdS quantum dots: new insights on CdS → lanthanide energy transfer mechanisms, *J. Mater. Chem.*, 2011, **21**(4), 1162–1170.

8 P. Mukherjee, R. F. Sloan, C. M. Shade, D. H. Waldeck and S. Petoud, A Postsynthetic Modification of II–VI Semiconductor Nanoparticles to Create Tb3+ and Eu3+ Luminophores, *J. Phys. Chem. C*, 2013, **117**(27), 14451–14460.

9 D. A. Chengelis, A. M. Yingling, P. D. Badger, C. M. Shade and S. Petoud, Incorporating Lanthanide Cations with Cadmium Selenide Nanocrystals: A Strategy to Sensitize and Protect Tb(III), *J. Am. Chem. Soc.*, 2005, **127**(48), 16752–16753.

10 J. K. Swabeck, S. Fischer, N. D. Bronstein and A. P. Alivisatos, Broadband Sensitization of Lanthanide Emission with Indium Phosphide Quantum Dots for Visible to Near-Infrared Downshifting, *J. Am. Chem. Soc.*, 2018, **140**(29), 9120–9126.

11 R. Marin and D. Jaque, Doping Lanthanide Ions in Colloidal Semiconductor Nanocrystals for Brighter Photoluminescence, *Chem. Rev.*, 2021, **121**(3), 1425–1462.

12 B. Zheng, J. Fan, B. Chen, X. Qin, J. Wang, F. Wang, R. Deng and X. Liu, Rare-Earth Doping in Nanostructured Inorganic Materials, *Chem. Rev.*, 2022, **122**(6), 5519–5603.

13 M. Liu, Z. Cai, Y. Xu, J. Hu and B. Sun, Europium(III)-Based Fluorescent Microspheres with Styrene Copolymerization toward an Enhanced Photoluminescence Performance, *ACS Appl. Polym. Mater.*, 2022, **4**(11), 8109–8117.

14 S. Susumu and W. Masanobu, Relations between Intramolecular Energy Transfer Efficiencies and Triplet State Energies in Rare Earth β-diketone Chelates, *Bull. Chem. Soc. Jpn.*, 1970, **43**(7), 1955–1962.

15 M. Latva, H. Takalo, V.-M. Mukkala, C. Matachescu, J. C. Rodríguez-Ubis and J. Kankare, Correlation between the lowest triplet state energy level of the ligand and lanthanide(III) luminescence quantum yield, *J. Lumin.*, 1997, **75**(2), 149–169.

16 J. Liu, K. Wang, W. Zheng, W. Huang, C.-H. Li and X.-Z. You, Improving spectral response of monocrystalline silicon photovoltaic modules using high efficient luminescent down-shifting Eu3+ complexes, *Prog. Photovoltaics*, 2013, **21**(4), 668–675.

17 M. D. McGehee, T. Bergstedt, C. Zhang, A. P. Saab, M. B. O'Regan, G. C. Bazan, V. I. Srdanov and A. J. Heeger, Narrow Bandwidth Luminescence from Blends with Energy Transfer from Semiconducting Conjugated Polymers to Europium Complexes, *Adv. Mater.*, 1999, **11**(16), 1349–1354.

18 K. Nakamura, Y. Hasegawa, H. Kawai, N. Yasuda, N. Kanehisa, Y. Kai, T. Nagamura, S. Yanagida and Y. Wada, Enhanced Lasing Properties of Dissymmetric Eu(III) Complex with Bidentate Phosphine Ligands, *J. Phys. Chem. A*, 2007, **111**(16), 3029–3037.

19 L. Aboshyan-Sorgho, C. Besnard, P. Pattison, K. R. Kittilstved, A. Aebischer, J.-C. G. Bünzli, A. Hauser and C. Piguet, Near-Infrared→Visible Light Upconversion in a Molecular Trinuclear d–f–d Complex, *Angew. Chem., Int. Ed.*, 2011, **50**(18), 4108–4112.

20 L. J. Charbonnière and N. Hildebrandt, Lanthanide Complexes and Quantum Dots: A Bright Wedding for Resonance Energy Transfer, *Eur. J. Inorg. Chem.*, 2008, **2008**(21), 3241–3251.

21 D. Geißler, S. Linden, K. Liermann, K. D. Wegner, L. J. Charbonnière and N. Hildebrandt, Lanthanides and Quantum Dots as Förster Resonance Energy Transfer Agents for Diagnostics and Cellular Imaging, *Inorg. Chem.*, 2014, **53**(4), 1824–1838.

22 R. A. Tigaa, G. J. Lucas and A. de Bettencourt-Dias, ZnS Nanoparticles Sensitize Luminescence of Capping-Ligand-Bound Lanthanide Ions, *Inorg. Chem.*, 2017, **56**(6), 3260–3268.

23 J. K. Molloy, C. Lincheneau, M. M. Karimdjy, F. Agnese, L. Mattera, C. Gateau, P. Reiss, D. Imbert and M. Mazzanti, Sensitisation of visible and NIR lanthanide emission by InPZnS quantum dots in bi-luminescent hybrids, *Chem. Commun.*, 2016, **52**(24), 4577–4580.

24 S. Miyazaki, K. Goushi, Y. Kitagawa, Y. Hasegawa, C. Adachi, K. Miyata and K. Onda, Highly efficient light harvesting of a Eu(III) complex in a host–guest film by triplet sensitization, *Chem. Sci.*, 2023, **14**, 6867–6875.

25 Y. Kitagawa, F. Suzue, T. Nakanishi, K. Fushimi, T. Seki, H. Ito and Y. Hasegawa, Stacked nanocarbon photosensitizer for efficient blue light excited Eu(III) emission, *Commun. Chem.*, 2020, **3**(1), 3.

26 V. Gray, P. Xia, Z. Huang, E. Moses, A. Fast, D. A. Fishman, V. I. Vullev, M. Abrahamsson, K. Moth-Poulsen and M. Lee Tang, CdS/ZnS core-shell nanocrystal photosensitizers for visible to UV upconversion, *Chem. Sci.*, 2017, **8**(8), 5488–5496.

27 L. Hou, A. Olesund, S. Thurakkal, X. Zhang and B. Albinsson, Efficient Visible-to-UV Photon Upconversion Systems Based on CdS Nanocrystals Modified with Triplet Energy Mediators, *Adv. Funct. Mater.*, 2021, **31**(47), 2106198.

28 Z. Huang and M. L. Tang, Designing Transmitter Ligands That Mediate Energy Transfer between Semiconductor Nanocrystals and Molecules, *J. Am. Chem. Soc.*, 2017, **139**(28), 9412–9418.

29 Z. Huang, Z. Xu, T. Huang, V. Gray, K. Moth-Poulsen, T. Lian and M. L. Tang, Evolution from Tunneling to Hopping Mediated Triplet Energy Transfer from Quantum Dots to Molecules, *J. Am. Chem. Soc.*, 2020, **142**(41), 17581–17588.

30 T. Huang, T. T. Koh, J. Schwan, T. T. T. Tran, P. Xia, K. Wang, L. Mangolini, M. L. Tang and S. T. Roberts, Bidirectional triplet exciton transfer between silicon nanocrystals and perylene, *Chem. Sci.*, 2021, **12**(19), 6737–6746.

31 Z. Xu, Z. Huang, C. Li, T. Huang, F. A. Evangelista, M. L. Tang and T. Lian, Tuning the Quantum Dot (QD)/Mediator Interface for Optimal Efficiency of QD-Sensitized Near-Infrared-to-Visible Photon Upconversion Systems, *ACS Appl. Mater. Interfaces*, 2020, **12**(32), 36558–36567.

32 H. Minami, N. Itamoto, W. Watanabe, Z. Li, K. Nakamura and N. Kobayashi, Chiroptical property enhancement of chiral Eu(III) complex upon association with DNA-CTMA, *Sci. Rep.*, 2020, **10**(1), 18917.

33 W. W. Yu, L. Qu, W. Guo and X. Peng, Experimental Determination of the Extinction Coefficient of CdTe, CdSe, and CdS Nanocrystals, *Chem. Mater.*, 2003, **15**(14), 2854–2860.

34 T. Jin, S. He, Y. Zhu, E. Egap and T. Lian, Bright State Sensitized Triplet Energy Transfer from Quantum Dot to Molecular Acceptor Revealed by Temperature Dependent Energy Transfer Dynamics, *Nano Lett.*, 2022, **22**(10), 3897–3903.

35 H. G. Brittain and F. S. Richardson, Circularly polarized emission studies on the chiral nuclear magnetic resonance lanthanide shift reagent tris(3-trifluoroacetyl-d-camphorato)europium(III), *J. Am. Chem. Soc.*, 1976, **98**(19), 5858–5863.

36 S. Maji and K. S. Viswanathan, Ligand-sensitized fluorescence of Eu3+ using naphthalene carboxylic acids as ligands, *J. Lumin.*, 2008, **128**(8), 1255–1261.

37 M. Mahboub, H. Maghsoudiganjeh, A. M. Pham, Z. Huang and M. L. Tang, Triplet Energy Transfer from PbS(Se) Nanocrystals to Rubrene: the Relationship between the Upconversion Quantum Yield and Size, *Adv. Funct. Mater.*, 2016, **26**(33), 6091–6097.

38 M. Mahboub, Z. Huang and M. L. Tang, Efficient Infrared-to-Visible Upconversion with Subsolar Irradiance, *Nano Lett.*, 2016, **16**(11), 7169–7175.

39 E. M. Rigsby, T. Miyashita, P. Jaimes, D. A. Fishman and M. L. Tang, On the size-dependence of CdSe nanocrystals for photon upconversion with anthracene, *J. Chem. Phys.*, 2020, **153**, 114702.

40 C. Mongin, P. Moroz, M. Zamkov and F. N. Castellano, Thermally activated delayed photoluminescence from pyrenyl-functionalized CdSe quantum dots, *Nat. Chem.*, 2018, **10**(2), 225–230.

41 K. Ravi Kumar, S. Satyen, S. Manjeev and M. Akhila, Photophysical Properties of 4-(Dicyanomethylene)-2-Methyl-6-(4-Dimethylaminostyryl)-4-H-Pyran (DCM) and Optical Sensing Applications, in *Photophysics,*

Photochemical and Substitution Reactions, ed. S. Satyen, K. Ravi Kumar and V. S. Tanja, IntechOpen, Rijeka, 2020, ch. 1.

42 Z. Huang, X. Li, B. D. Yip, J. M. Rubalcava, C. J. Bardeen and M. L. Tang, Nanocrystal Size and Quantum Yield in the Upconversion of Green to Violet Light with CdSe and Anthracene Derivatives, *Chem. Mater.*, 2015, **27**(21), 7503–7507.

43 T. Miyashita, P. Jaimes, T. Lian, M. L. Tang and Z. Xu, Quantifying the Ligand-Induced Triplet Energy Transfer Barrier in a Quantum Dot-Based Upconversion System, *J. Phys. Chem. Lett.*, 2022, **13**(13), 3002–3007.

44 Z. Huang, P. Xia, N. Megerdich, D. A. Fishman, V. I. Vullev and M. L. Tang, ZnS Shells Enhance Triplet Energy Transfer from CdSe Nanocrystals for Photon Upconversion, *ACS Photonics*, 2018, **5**(8), 3089–3096.

45 K. Wu, Y. Du, H. Tang, Z. Chen and T. Lian, Efficient Extraction of Trapped Holes from Colloidal CdS Nanorods, *J. Am. Chem. Soc.*, 2015, **137**(32), 10224–10230.

46 H. Zhu, Y. Yang, K. Hyeon-Deuk, M. Califano, N. Song, Y. Wang, W. Zhang, O. V. Prezhdo and T. Lian, Auger-assisted electron transfer from photoexcited semiconductor quantum dots, *Nano Lett.*, 2014, **14**(3), 1263–1269.

47 X. Luo, Y. Han, Z. Chen, Y. Li, G. Liang, X. Liu, T. Ding, C. Nie, M. Wang, F. N. Castellano and K. Wu, Mechanisms of Triplet Energy Transfer Across the Inorganic Nanocrystal/Organic Molecule Interface, *Nat. Commun.*, 2020, **11**(1), 28.

48 Y. Han, X. Luo, R. Lai, Y. Li, G. Liang and K. Wu, Visible-Light-Driven Sensitization of Naphthalene Triplets Using Quantum-Confined CsPbBr3 Nanocrystals, *J. Phys. Chem. Lett.*, 2019, **10**(7), 1457–1463.

49 S. He, X. Luo, X. Liu, Y. Li and K. Wu, Visible-to-Ultraviolet Upconversion Efficiency above 10% Sensitized by Quantum-Confined Perovskite Nanocrystals, *J. Phys. Chem. Lett.*, 2019, **10**(17), 5036–5040.

50 H. Lu, X. Chen, J. E. Anthony, J. C. Johnson and M. C. Beard, Sensitizing Singlet Fission with Perovskite Nanocrystals, *J. Am. Chem. Soc.*, 2019, **141**(12), 4919–4927.

51 S. Garakyaraghi, C. Mongin, D. B. Granger, J. E. Anthony and F. N. Castellano, Delayed Molecular Triplet Generation from Energized Lead Sulfide Quantum Dots, *J. Phys. Chem. Lett.*, 2017, **8**(7), 1458–1463.

52 Y. Sang, J. Han, T. Zhao, P. Duan and M. Liu, Circularly Polarized Luminescence in Nanoassemblies: Generation, Amplification, and Application, *Adv. Mater.*, 2020, **32**(41), 1900110.